Taylor & Francis
Taylor & Francis Group

ARTICLE

Check for updates

Physically motivated lumped-parameter model for proportional magnets

Olivier Reinertz

Institute for Fluid Power Drives and Systems (IFAS), RWH Aachen University, Aachen, Germany

ABSTRACT

The paper presents a novel physically motivated lumped-parameter model for one-dimensional simulation of proportional magnets. The model is deduced by analysing the significant physical interactions, properties of state-of-the art actuators and limitations of contemporary lumped-parameter models. The resulting model equations are taking into account the main properties of commonly used proportional magnets in the relevant field of operation, as e.g. nonlinear force and flux linkage characteristics over stroke and current, and are respecting the dominant physical effects, leading to these nonlinearities and linking the two before mentioned characteristics. This enables not only the parameterisation by a small number of independent parameters, but also physically correct parameter studies. After the model's ability to describe the static behaviour of proportional magnets is proven by using measurement data of two off-the-shelf actuators, the paper concludes with a dynamic model validation, highlighting the good accuracy of the modelled frequency response.

Introduction

The rising number of electro-hydraulic controls and the increasing complexity of control algorithms, disclosed e.g. by Burget and Weber (2012), require simulation-based studies including the electromechanical interfaces. This leads to a demand for precise lumped-parameter models of electro-proportional valve actuators which are taking into account the electrical and mechanical behaviour and thus linking electric control and hydraulics. Proportional magnets are widely used as such actuators for common control valves. Nevertheless, accurate and physically motivated models, which describe the dominant effects by use of only few independent parameters and thus allow physically correct parameter studies, are not available. In the scope of this paper, first the fundamentals of electromagnetism and proportional magnets are presented. Furthermore, state-of-the-art lumped-parameter models are introduced and compared with respect to accuracy, parameterisation effort and the ability to realise required parameter studies by use of independent parameters. Subsequently, a novel model meeting the above-mentioned requirements is derived and validated with measurement results.

Fundamentals of electromagnetism

Electromagnetic actuators convert the supplied electric energy into mechanical energy, magnetic energy and heat. The magnetic energy is stored in the magnetic field while dissipation is due to hysteresis losses and the ohmic resistance of the coil R. The supplied energy W can be calculated out of the supplied voltage $u(t)$ and current $i(t)$ by Equation 1. Moreover, assuming that hysteresis effects may be neglected, the energy stored in the magnetic field W_{mag} can be calculated out of the electrical signals, current $i(t)$ and inductive voltage $u_L(t)$, by using Equations 2 and 3. Herein, the inductive voltage equals the time derivative of the magnetic flux linkage $\lambda(t)$. The magnetic flux linkage describes the total magnetic flux passing the surface spanned by the coil's windings multiplied with its number of turns. It is an integral parameter of the magnetic field describing the interaction of electric, magnetic and mechanical system. For electromagnetic actuators, it depends on the supplied current and the actuator's stroke as well as on their history due to material hysteresis, fringing effects and eddy current losses.

$$W = \int_0^t u(t) \cdot i(t) dt \tag{1}$$

$$u(t) = i(t) \cdot R + \frac{d\lambda}{dt} = i(t) \cdot R + u_L(t) \tag{2}$$

$$W_{mag}(t) = \int_0^t u_L(t) \cdot i(t) dt = \int_0^t \frac{d\lambda(t)}{dt} \cdot i(t) dt$$
$$= \int_0^t i(t) d\lambda(t) \tag{3}$$

CONTACT Olivier Reinertz ✉ Olivier.reinertz@ifas.rwth-aachen.de 🖃 Institute for Fluid Power Drives and Systems (IFAS), RWH Aachen University, Campus Boulevard 30, Aachen D-52074, Germany

By neglecting the above-mentioned hysteresis effects, the velocity of change and thus the voltage and current course over time are irrelevant and Equation 3 can be written as a function of armature position x and flux linkage λ:

$$W_{\mathrm{mag}}(x, \lambda) = \int_0^\lambda i(x, \lambda) d\lambda \quad (4)$$

As has been shown, e.g. by Roters (1941), when moving the armature at a constant supply current i_0 of the coil, the performed mechanical work W_{mech} equals the sum of the change in stored magnetic energy by the movement and the additionally supplied magnetic energy ΔW_{mag} during motion due to energy conservation. Herein, the additional magnetic energy results from a change in magnetic flux linkage λ and thus a nonzero u_L over the stroke. Considering the flux linkage λ_0 in the starting position x_0, the change in position Δx and the change in flux linkage $\Delta \lambda$ due to the movement, the mechanical work is calculated by

$$W_{\mathrm{mech}} = W_{\mathrm{mag}}(x_0, \lambda_0) - W_{\mathrm{mag}}(x_0 + \Delta x, \lambda_0 + \Delta \lambda) + \Delta W_{\mathrm{mag}}(\Delta x, \Delta \lambda)$$

$$W_{\mathrm{mech}} = \int_0^{\lambda_0} i(x_0, \lambda) d\lambda - \int_0^{\lambda_0 + \Delta \lambda} i(x_0 + \Delta x, \lambda) d\lambda + \int_{\lambda_0}^{\lambda_0 + \Delta \lambda} i_0 d\lambda \quad (5)$$

The method of integration by parts allows the rearrangement of this equation leading to the following equation:

$$W_{\mathrm{mech}} = -\int_0^{i_0} \lambda(x_0, i) di + \int_0^{i_0} \lambda(x_0 + \Delta x, i) di \quad (6)$$

Finally, the consideration of an infinitely small change in position yields the direct relation between force and flux linkage in Equation 7, which may be found in, e.g. Kallenbach et al. (2012),

$$F(x, i) = \frac{\partial}{\partial x} \int_0^i \lambda(x, i) di \quad (7)$$

The combination of Equation 7 with Equation 2 allows physically motivated modelling of valve actuators including their interaction with electrical and mechanical subsystems. Nevertheless, the magnetic flux linkage resulting from a magnetic field exerted by the driving current $i(t)$ in a coil possessing N windings and from the magnetic resistance of the system R_M must be known in the full stroke and current regime, which is rarely the case for off-the-shelf actuators.

In general, the magnetic flux linkage can be calculated by Equation 8. The magnetic resistance of the system is influenced by the air gap length, saturation

effects of the conducting material and stray flux leading to a stroke and current-dependent behaviour. Unfortunately, the magnetic resistance is rarely known in detail, hindering a direct calculation of the flux linkage out of this equation for most applications:

$$\lambda(x, i) = \frac{N \cdot i(t)}{R_M(x, i)} \quad (8)$$

Nevertheless, in the special case of a system working at low flux densities in soft iron material at sufficient air gap lengths and with negligible stray flux, the magnetic resistance of the system is dominated by the air gap and thus is proportional to its length $(x_{\mathrm{max}} - x(t))$. Thus, considering an air gap with constant cross section A and permeability μ_0, the quadratic reluctance force in Equation 9 is obtained:

$$\lambda(x, i) = \frac{N \cdot i(t)}{R_M(x)} = \frac{N \cdot i(t) \cdot \mu_0 \cdot A}{x_{\mathrm{max}} - x(t)} \Rightarrow F$$
$$= \frac{N \cdot i(t)^2 \cdot \mu_0 \cdot A}{2 \cdot (x_{\mathrm{max}} - x(t))^2} \quad (9)$$

In summary, the ohmic resistance and the dynamics of the magnetic flux characterise the magnetic force and the electric behaviour of the system, so that a physically motivated modelling of an actuator should primarily focus on the magnetic flux characteristics over stroke and current and its dynamics. Unfortunately, its highly nonlinear behaviour is difficult to measure and calculate in all stroke positions and thus is not available for off-the-shelf actuators in the field, so that modelling approaches out of the static magnetic force characteristics are of special interest.

Properties of proportional magnets

Electro-proportional valves are mostly using proportional magnets to control the desired output by balancing the exerted magnetic force with a process force which linearly depends on the controlled output. Herein, the process force may be generated by a mechanical spring to control the valve spool's position in directional valves and/or by pressures acting on control faces to control the pressure as well in electromechanically controlled pressure relief and reducing valves as in flow control valves. In all of these valves linear control behaviour is intended, which leads to the requirement that the magnetic force needs to be proportional to the applied electrical current and almost independent of the armature position. Additional information on the control behaviour of proportional valves may be found in, e.g., Backé and Klein (2004).

Proportional magnets are realised by shaping the magnetic resistance over the stroke and coil current.

The main optimisation goal is a proportionality of force and current as well as an almost stroke independent behaviour, both optimising controllability of the valve. Tuning of the magnetic resistance is achieved by use of, e.g. chamfers, additional air gaps or conical nonmagnetic rings and soft iron materials of specific quality, to approximate the idealised behaviour in the following equation:

$$F(i) = k_0 \cdot i \qquad (10)$$

By use of Equation 7 and the monotonically rising integration constant $\lambda_0(i)$ describing the flux linkage in the initial position, the flux linkage for the above-stated idealised force relationship can be deduced as follows:

$$\lambda(x, i) = \lambda_0(i) + k_0 \cdot x \qquad (11)$$

This equation shows unphysical behaviour as a magnetic flux occurs at nonzero armature positions while no electric current is applied. Hence, a proportional magnet will never achieve the idealised behaviour in Equation 10 and a more sophisticated model needs to be implemented.

In the following, results of an electromagnetic 3D-finite element analysis of an arbitrary chosen proportional magnet are analysed to understand the significant limitations in flux shaping and thus in operational behaviour of proportional magnets.

Reference data

As a reference, the exemplary geometry of a single acting proportional magnet comparable to the one used by Schultz and Tappe (2006) is used. All simulations were carried out in Altair Flux™. The geometry is depicted in Figure 1. In the origin, the air gap is closed and $x = 0$.

Figure 2 shows the force and flux characteristics of the simulated proportional magnet. The grey parts correspond to the working range and thus the relevant part for model development. It becomes obvious that at low driving currents, the exerted force is strongly nonlinear.
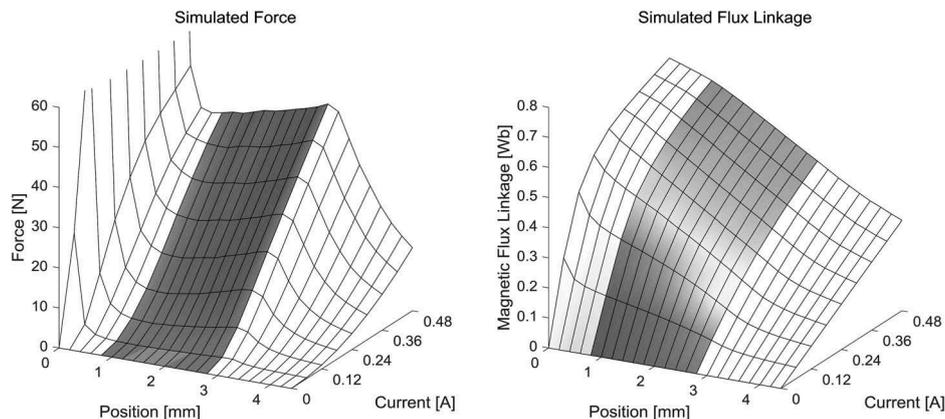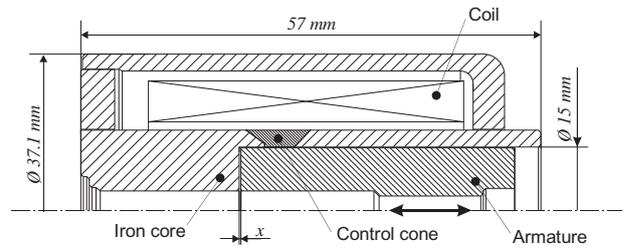

Figure 1. Half-section of the reference geometry.

This can be explained by the fact that by reducing the magnetic flux linkage by additional air gaps and cones, the parabolic behaviour in Equation 9 and thus a zero slope at zero current cannot be avoided. Position has only a small influence on the exerted force, but this should also be considered for model development to improve its accuracy and applicability. The right diagram shows, that at higher position values, a linear correlation of current and magnetic flux, and thus a constant inductance exists. This is due to the fact that the resistance of the air gap dominates the resulting magnetic resistance of the system. But already at position 2.8 mm, which is the highest air gap in the working area, nonlinear behaviour can be observed and has to be enclosed in the model.

State-of-the-art models

In the following section, different approaches for modelling proportional magnets with lumped parameters are introduced and discussed. First, it may be distinguished between two different fundamental model structures. These are using different approaches to calculate out of the change in flux linkage through the coil $d\lambda/dt$ the coil current i. Figure 3 shows the first-model structure, which uses the partial differentials $\delta\lambda/\delta x$ and $\delta\lambda/\delta i$ in the actual point of operation, defined by x and i, to calculate di/dt out of $d\lambda/dt$ and dx/dt. Thus, the electric current is achieved by integrating its derivative.
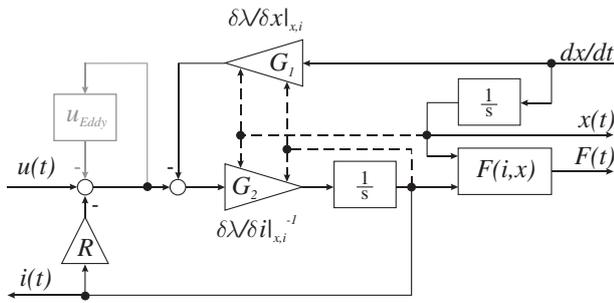

Figure 2. Simulated characteristics of the reference system.

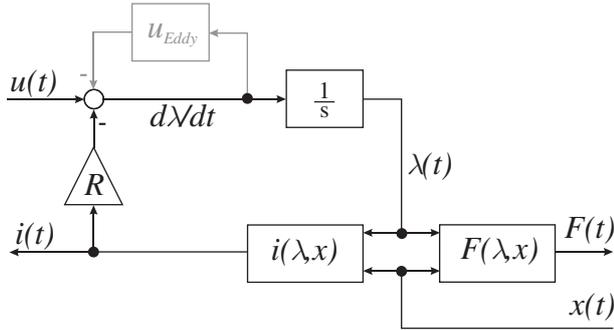**Figure 3.** First-model structure for electromagnet simulation.

Figure 4. Second-model structure for electromagnet simulation.

In the second-model structure, which is shown in Figure 4, the magnetic flux λ is determined by integrating the inductive voltage u_L and thus its time derivative, while the current is directly calculated out of a two-dimensional characteristic map or equation depending on actual magnetic flux λ and position x.

Based on these two structures, a multitude of models can be generated differently describing the magnetic flux and its partial derivatives and dynamic hysteresis due to eddy currents and field propagation. Selected widely used models are discussed in the following.

Model A: Vaughan and Gamble model

The empirical model described by Vaughan and Gamble (1996) is widely used in literature. The model bases on a publication of Chua and Stromsmoe (1970) on lumped-parameter modelling of nonlinear inductors focusing on periodic signals. The model uses integration of the inductive voltage and thus the second-model structure in Figure 4 for calculating the electric current.

Nevertheless, contrary to the scheme in Figure 4, this model considers not only an energy-restoring part $i_R(t)$ of the current which depends on actual magnetic flux linkage and position, but also dynamic hysteresis effects due to eddy currents. This is achieved by adding to the energy-restoring part $i_R(t)$ an energy-dissipating part $i_d(t)$ summing up to the total supply current $i(t)$. This means for the modelling of the electric circuit a parallel arrangement of restoring and dissipating path of the coil is present:

$$i(t) = i_R(t) + i_d(t) \tag{12}$$

The restoring part of the current is considered in the model by means of the two-dimensional polynomial in Equation 13, which depends on the actual stroke $x(t)$ and magnetic flux linkage $\lambda(t)$. For the definition of its coefficients $pi_{n,m}$, measurements of the magnetic flux linkage over supplied current in discrete positions have to be performed. The indirectly measured flux linkage is calculated using Equation 14 by time-wise integration of the measured inductive voltage $u_L(t)$, which has first to be corrected from hysteresis:

$$i_R(t) = \sum \left(\sum pi_{n,m} \cdot x(t)^m \right) \cdot \lambda(t)^n \tag{13}$$

$$\lambda(t) = \int u(t) - i(t) \cdot R \, dt = \int \overline{u_L(t)} \, dt \tag{14}$$

$$i_d(t) = h(u_L(t), t) \tag{15}$$

Contrary to this, the model for the energy-dissipating current $i_d(t)$ directly depends on the inductive voltage $u_L(t)$ and thus on $d\lambda/dt$. The describing equation has to be adapted to the system so that realistic eddy current losses and thus hysteresis loops are achieved. Therefore, different polynomial approximation functions are used in literature. These have to be monotonically rising and have to cross the origin, so that under static condition, the dissipating current equals zero. Moreover, Zavarehi and Lawrence (1999) use a first-order element, in addition to a polynomial function, to consider dynamic effects resulting from magnetic field propagation in the core.

For the calculation of the magnetic force, the model also uses a polynomial approximation function, which is not linked to the functions for the electrical system. The grade of this polynomial function has again to be tuned on the behaviour of the investigated system. Dell'Amico (2016), for example, uses this approach with 16 nonzero coefficients $pfs_{n,m}$ in Equation 16. In contrast to this, the original model of Vaughan and Gamble includes only a one-dimensional polynomial depending on λ^2 which in turn is both stroke and current dependent:

$$F(i, x) = \sum \left(\sum pfs_{n,m} \cdot x^m \right) \cdot i^n \tag{16}$$

Cristofori and Vacca (2012) implemented an additional hysteresis model for modelling static hysteresis in the magnetic circuit resulting from residual magnetism, which is not influencing the electromagnetic properties, but the force build-up.

In conclusion, this method leads to very accurate simulation models if polynomial functions of sufficient order are used and carefully parameterised. A suitable parameterisation guideline was published by Zavarehi

and Lawrence (1999), ensuring very accurate model parameterisation. Nevertheless, the required effort for measurement and parameterisation is still comparably high.

Besides this high effort for measuring the required data and subsequent parameter estimation, the above-mentioned dependencies between the describing functions for force and restoring current are not considered. In the case of parameter studies, this may lead to unphysical behaviour, as the existing dependencies between the available tuning parameters are not covered by the model and unphysical combinations are not supressed.

Hence, a compromise with lower parameterisation effort needs to be found in the following that possesses, besides a good accuracy, physically independent parameters to avoid unphysical combinations in parameter studies.

Model B: characteristic maps

The use of multiple characteristic maps describing the electromagnetic system is another widely used approach. Recent examples of application can be found, e.g., in Ruderman and Gadyuchko (2013), Krimpmann *et al.* (2016) and Meng *et al.* (2016). In both model structures mentioned earlier, a map is used to model the force depending on the core position and either on the actual flux linkage or on electric current, while one or more additional tables allow the static characterisation of the magnetic flux linkage. With the first-model structure in Figure 3, this is achieved by characteristic maps for $d\lambda/dt$ and $\delta\lambda/\delta x$, the partial differentials of the flux linkage, while in the second case, a characteristic map for restoring current is required.

Especially the calculation of the above-mentioned differentials out of measurement data can be numerically challenging, so characteristic maps are mostly used with the second-model structure in Figure 4. The implementation of eddy currents is in most cases realised by means of a series arrangement of an additional resistor and partially by an inductance in the electric circuit in parallel to the inductance of the coil to model the time behaviour of the field propagation. Also by characteristic maps, the energy conservation and thus Equation 7 are not used to reduce parameterisation effort and to enable physically correct parameter studies.

Model C: linearised model

A linearisation of both above-mentioned models leads again to the description of an idealised proportional magnet, as has been shown in Equations 10 and 11. Such a linearised model, used e.g. by Huayong *et al.* (2009) and by Cristofori and Vacca

(2012) for a small-signal approach, possesses a proportionality of force and current while the force is not affected by the armature position. Moreover, proportionality between magnetic flux and current is assumed and described by using the inductance L.

This yields the non-physical model in Equations 17 to 19, which allows simple parameterisation, small calculation times and the development of control schemes by linear control technique:

$$F(i) = k_0 \cdot i \qquad (17)$$

$$\lambda(x,i) = L \cdot i + k_0 \cdot x \qquad (18)$$

$$u(t) = i(t) \cdot R + L\frac{di(t)}{dt} + k_0\frac{dx(t)}{dt} \qquad (19)$$

The parameter k_0 is calculated out of one data couple for force and current and describes the force gain over current as well as the velocity-dependent mutual inductance of the system. The ohmic resistance R can be measured by means of an RLC meter, while the inductance should be measured in the operating point. The equations above are arranged for use in the first-model structure. Nevertheless, due to its simplicity, this model may be used with both previously shown model structures by rearranging the equations accordingly. Due to the linearisation, this model represents measurement results only in a small field of application with sufficient accuracy.

Development of a novel physically motivated model

The development of this novel model aims to achieve a simple to use mathematical representation of proportional magnets, which is physically motivated and thus reducing the effort for parameterisation compared to mostly phenomenological approaches while enabling physically correct parameter studies. Taking a closer look on Equation 7, it becomes obvious that by providing a characteristic map of the stroke- and current-dependent magnetic flux linkage, the force characteristic is defined as well. Unfortunately in most cases, the flux characteristic is not available, so an inverse approach focusing on the exerted force is favourable. Therefore, Equation 7 has to be rearranged:

$$\lambda(x,i) = \frac{\partial}{\partial i}\int_0^x F(x,i)dx + \lambda_0(i) \qquad (20)$$

The use of Equation 20 poses the following challenges for model development:

- In general, a description of the force over the full stroke and current regime $F(x, i)$ is not available.
- Usage of Equation 20 requires knowledge on the integration constant $\lambda_0(i)$.

Hence, an adequate approximation function for the force $F(x, i)$ has first to be developed, respecting the physical restrictions for the force as well as for the magnetic flux linkage while being defined by only a few datapoints. Considering the above-stated Equation 20 and additionally Equation 9, a series of properties can be deduced for negligible driving currents, and thus at a current-independent magnetic resistance R_M. Moreover, at higher driving currents, the aspired proportional behaviour has to be taken into account. As may be seen in Figure 2, real systems always possess a certain offset from proportional behaviour, as the slope at small currents is limited and thus smaller than aspired. The slope of the force over current should be constant at higher driving currents to achieve proportional behaviour. However, usually a stroke dependency occurs. Table 1 summarises these requirements.

The mathematical representation of the obviously changing order of the force equation over current can be achieved by use of a switching function $f(n, i)$ in the current–force relationship. The polynomial function $k(x)$ handles the stroke dependency of the force. By this, the force and flux linkage can be calculated by the following set of equations:

$$\begin{cases} F(x,i) = f(n,i) \cdot i \cdot k(x) \\ \lambda(x,i) = \lambda_0(i) + \left(f(n,i) + \frac{\partial f(n,i)}{\partial i} \cdot i \right) \cdot \int_0^x k(x)dx \end{cases} \tag{21}$$

To allow comparable results with constant $k(x)$, the different switching functions $f(n, i)$ are normalised. Their gain in the origin is n and their limit at high currents is 1. Table 2 gives an overview on different normalised switching functions used for model development.

The integration constant $\lambda_0(i)$ in Equation 20 or 21, respectively, represents the magnetic flux linkage in the origin. The location of the origin can be arbitrarily defined. At low currents, a constant inductivity L_0 can be assumed so that the flux

linkage is proportional to the current, while at higher currents saturation effects occur and, as a rough estimate, limit the flux linkage to a constant value $\lambda_{\max}$. This effect is described by Equation 22 basing also on a switching function $g(L_0/\lambda_{\max}, i)$ for description of the switching from proportional to constant behaviour:

$$\lambda_0(i) = \lambda_{\max} \cdot g\left(\frac{L_0}{\lambda_{\max}}, i \right) \tag{22}$$

Finally, for dynamic simulation, the following set of Equations 23 can be used, which is based on the first-model structure. As the inverse function of the flux linkage is not available, the use of the second-model structure is not feasible:

$$\begin{cases} F(x,i) = f(n,i) \cdot i \cdot k(x) \\ \frac{\partial \lambda(x,i)}{\partial x} = \left(f(n,i) + \frac{\partial f(n,i)}{\partial i} \cdot i \right) \cdot k(x) \\ \frac{\partial \lambda(x,i)}{\partial i} = \frac{\partial \lambda_0(i)}{\partial i} + \left(2\frac{\partial f(n,i)}{\partial i} + \frac{\partial^2 f(n,i)}{\partial i^2} \cdot i \right) \cdot \int^k (x)dx \\ \frac{di(t)}{dt} = \frac{u(t) - i(t) \cdot R - \frac{\partial \lambda(x,i)}{\partial x} \cdot \frac{dx(t)}{dt}}{\frac{\partial \lambda(x,i)}{\partial i}} \\ i(t) = \int \frac{di(t)}{dt} dt \end{cases} \tag{23}$$

To include eddy current losses in the magnetic circuit, the method used by other models described in the previous section can be applied. Hence, the total current on the driving ports of the coil is raised by an additional resistance in parallel to the coil inductance.

Parameterisation

The model parameters in Table 3 are required for simulation. While the ohmic resistance R can be measured directly, all other values have to be indirectly determined by calculation out of measurement data. Assuming the polynomial

$$k(x) = k_0 + \sum k_m \cdot x^m \text{ with } m \in \mathbb{N}_{[0]} \tag{24}$$

is used, the simplest way for parameterisation of n and the constant k_0 of the polynomial is to use two data couples consisting of force and current in position $x = 0$. By this, all other terms of the polynomial $k(x)$ are zero and the two remaining model parameters can easily be defined.

The origin of the coordinate system can be chosen depending on the application and on available

Table 1. Required model properties.

Current	Force	Magnetic flux linkage
$i = 0$	$F = 0$; $\delta F/\delta i = 0$	$\lambda = 0$; $\lambda_0 = 0$
$i \to 0$	$F \sim i^2$; $\delta F/\delta i \sim i$	$\lambda \sim i$
$i \gg 0$	$\delta F/\delta i = k(x)$	

Table 2. Normalised switching functions and corresponding differential terms.

Switching function $f(n,i)$ or $g(n,i)$	$f(n,i) + \frac{\partial f(n,i)}{\partial i} \cdot i$
$\text{erf}\left(\frac{\sqrt{\pi}}{2} n \cdot i \right)$	$\text{erf}\left(\frac{\sqrt{\pi}}{2} n \cdot i \right) + \left(\frac{\sqrt{\pi}}{2} n \cdot i \right) \cdot e^{-\left(\frac{\sqrt{\pi}}{2} n \cdot i \right)^2}$
$\tanh(n \cdot i)$	$\tanh(n \cdot i) + \frac{4n \cdot i}{(e^{n \cdot i} + e^{-n \cdot i})^2}$
$\frac{2}{\pi} \text{atan}\left(\frac{\pi}{2} n \cdot i \right)$	$\frac{2}{\pi} \text{atan}\left(\frac{\pi}{2} n \cdot i \right) + \frac{4n \cdot i}{4 + (\pi \cdot n \cdot i)^2}$
$\frac{n \cdot i}{(1 + n^K \cdot i^K)^{\frac{1}{K}}}$	$\frac{2n \cdot i + n^{K+1} \cdot i^{K+1}}{(1 + n^K \cdot i^K)^{\frac{K+1}{K}}}$

Table 3. Model parameters.

Parameter	Determination
R	RLC meter
L_0	RLC meter
n	Static force characteristic @ $x = 0$
k_0	Static force characteristic @ $x = 0$
$k_{1\ldots n}$	Static force characteristic @ $x \neq 0$
$\lambda_{\max}$	Step response or measurement of $\lambda_0(i)$ @ $x = 0$

measurement data. When modelling pressure valves for example, the origin may be set to the static armature position at zero flow. Thus, the force characteristic in $x = 0$ can be determined by using the control face areas and measuring the controlled pressure over current. For directional valves, the highest air gap length is most suitable.

Thus, the reference position is reached at zero current.

The required approximation functions are summarised in Table 4. The switching function $f(n, i)$ can be chosen according to the system behaviour. Table 2 gives an overview of such functions. Model accuracy can be improved by changing the course of the force build-up. In most of the cases, the switching function $f(n, i) = \tanh(n \cdot i)$ represents the force build-up over current with best accuracy, so that it is exclusively used in the following examples for modelling the force build-up.

The polynomial $k(x)$ describes the course of the force over the stroke. Thus, its behaviour must be determined by use of additional data for different air gap lengths. It can be set constant for proportional magnets with negligible influence of the stroke on the force, which are widely used in directional valves.

To allow for a good parameterisation of n and $k(x)$, datapoints should be gained out of static force measurements. Herein, hysteresis effects and resulting measurement inaccuracies have to be considered. These would directly result in model inaccuracies of the same magnitude, especially when parameterising n and $k(x)$ with only few datapoints. Therefore, all force measurements should be repeated after a rising and falling current and stroke, to minimise the impact of hysteresis effects on model accuracy. By averaging all results for a datapoint hysteresis and measurement noise are reliably cancelled.

The inductance L_0 should ideally be determined by measuring the inductance at small currents in the origin of the stroke coordinate. Nevertheless, if this is not feasible, it can be measured in another position x_M in the working stroke. In this case, the following equation is used for converting the measured value L_M into L_0:

$$L_0 = L_M - \int_0^{x_M} k(x) dx \qquad (25)$$

Finally, determination of the parameter λ_{max} and the switching function $g(L_0/\lambda_{max}, i)$ defines the course of $\lambda_0(i)$ and thus of the differential inductance over

current. The equation for g and its parameter λ_{max} are also referenced on the stroke origin previously defined. Parameterisation can be achieved by measurement of the current-dependent magnetic flux linkage or by fitting the behaviour of the actuator on step responses. In most of the cases, the switching function $g = 2\lambda_{max}/\pi \cdot \text{atan}(\pi/2 \cdot n \cdot i)$ is best suited and thus used for all following model validations.

Model validation

The validation process is divided into three steps. First, the static force and flux linkage of lumped-parameter model and reference data are compared. Second, the model is used to approximate two different static force characteristics of measured proportional magnets by means of the presented parameterisation rules. Finally, the dynamic behaviour of both measured devices is compared with the dynamic model properties, to show the ability of the model, to predict the actuator's dynamics out of the static force and few additional parameters.

As a first model check, its results are compared to the simulated static reference data. Figures 5 and 6 represent the results of the model in absolute values of force and magnetic flux linkage, as well as their deviation to reference data by colour scale in the working area. A positive deviation represents an overestimation of the model compared to the reference data. It is obvious that in a wide stroke regime, good accordance in force as well as in flux linkage is achieved. Thus, the previously shown model is capable of representing the reference system with sufficient accuracy. For the polynomial $k(x)$, a first-order equation with small gain is used, as the magnet shows almost linear behaviour in the working regime.

Further, the model is validated by means of measurements. Therefore, the static force characteristics of two different actuators were measured. Due to inevitable hysteresis, caused by friction and magnetic hysteresis of the iron parts, the mean value of the measurement data at rising and falling current is used in the following for model parameterisation and validation. The processed measurement results are shown in Figure 7. The first tested device, displayed on the left, shows approximately linear behaviour in its working stroke from 0.5 to 2.5 mm. Out of the working stroke, strong nonlinearities occur, so that these regimes should be avoided by design measures in a real valve. The model parameterisation therefore focuses on the working stroke highlighted in grey. The second tested device possesses a working stroke of 0 to 2 mm which has to be modelled. In this stroke regime, the actuator's force behaves nonlinear, so that this curvature has to be taken into account by an appropriate order of $k(x)$ and its parameterisation.

Table 4. Approximation functions.

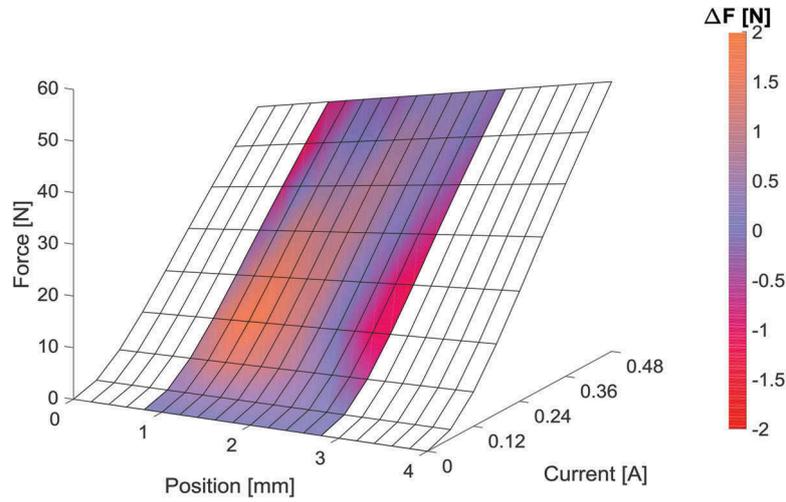| Model functions	Determination
$f(n, i)$	$F(i)$ @ $x = 0$
$k(x)$	$F(x)$ @ $x \neq 0$, $i =$ const.
$g(L_0/\lambda_{max}, i)$	Step response

Figure 5. Result of a lumped-parameter model for reference data; colour: deviation to reference data.
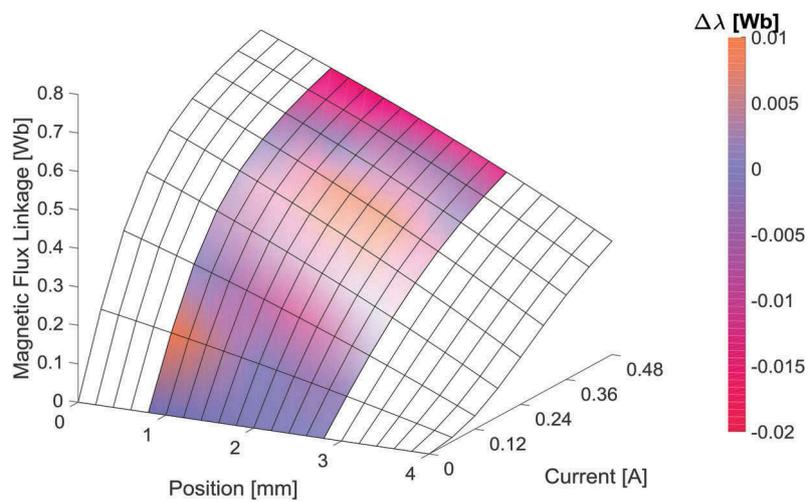

Figure 6. Result of a lumped-parameter model for reference data; colour: deviation to reference data.
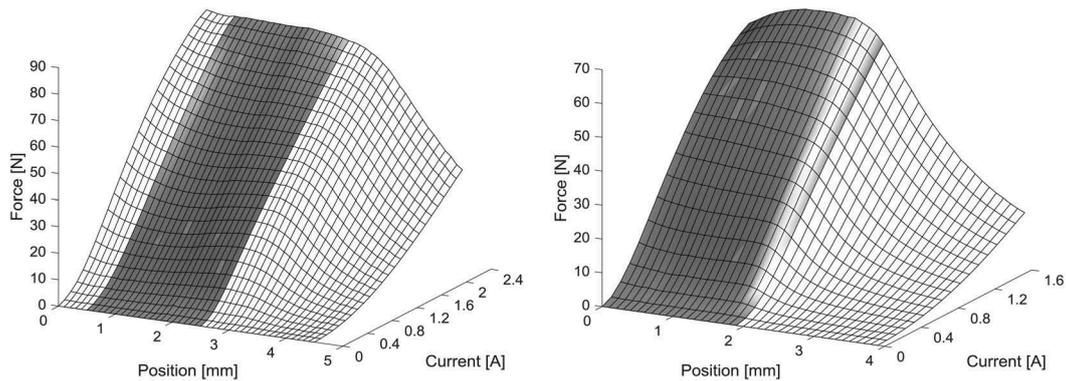

Figure 7. Measured reference data; left: test device 1, right: test device 2.

By means of the presented model parameterisation rules, all parameters are set and the deviations of measured and simulated forces in steady state are depicted in Figures 8 and 9 for both actuators. Please note that colour scales of Figures 4, 7 and 8 are differing to ensure good

visibility of the resulting deviations between measurements and models.

All presented models are based on a $\tanh(ni)$ switching function for the force build-up. The degree m of $k(x)$ varies depending on the shape of the force characteristics. In the case of the reference model and test device 1, a
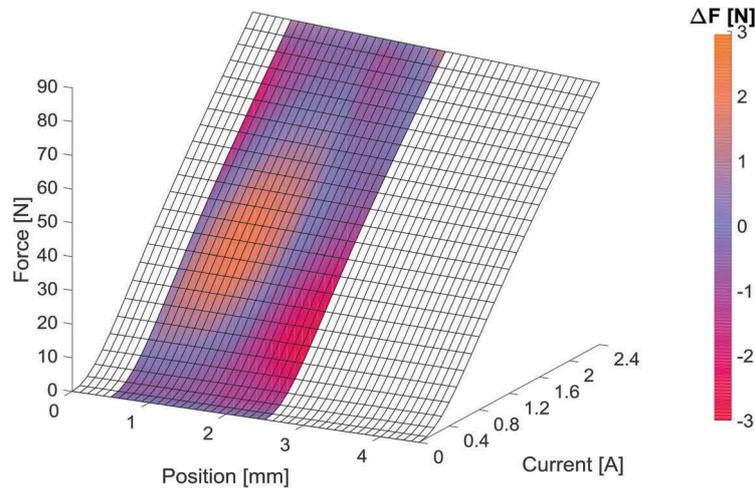
Figure 8. Result of a lumped-parameter model for device 1; colour: deviation to measurement.
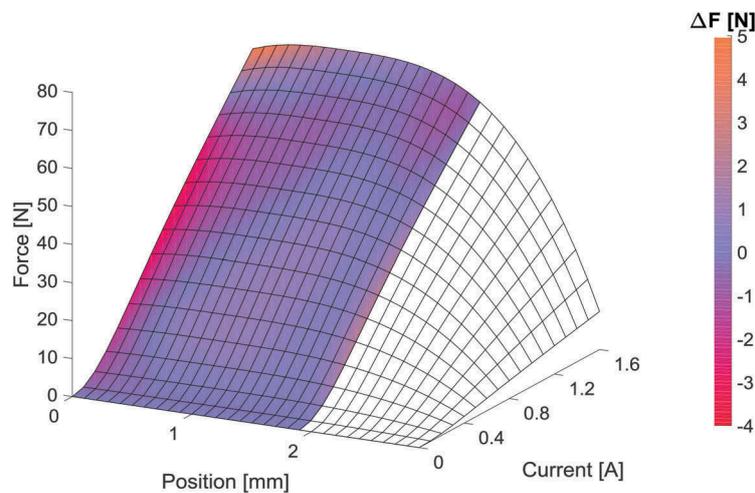
Figure 9. Result of a lumped-parameter model for device 2; colour: deviation to measurement.

linear correlation is used while in case of test device 2, a third-order polynomial needs to be applied. Slightly higher inaccuracies occur in the case of test device 2 on the left border of the characteristics. Nevertheless, in the main operating area good accordance between measurement data and model is achieved.

A MATLAB Simulink model based on the set of Equations 23 is used to compare dynamic measurements with simulation results. Measurements were performed by operating the proportional magnets against a pre-tensioned spring, resulting in a dynamic system comparable to common valves.

Parameterisation of dry friction occurring at the interface between armature and iron core during the measurement poses a big challenge for isolated validation of a magnetic model. This friction forces are the result of inevitable magnetic radial forces between armature and iron core, due to asymmetric radial flux resulting from design, a dislocation of the armature in its guidance and production tolerances. Hence, this radial magnetic force depends on the stroke as well as on the flux. It can hardly be described without

a deeper knowledge on the unknown geometry, tolerances and materials of the device. Therefore, the model only includes a constant friction force and is validated with harmonic signals, keeping the armature continuously in motion to avoid standstill and thus stick-slip effects. The frequency response diagrams in the following are based on measurements with harmonic excitations for distinct frequencies. The driving voltage signals of the measurements with amplitudes of approximately 0.5 V for the first device and 1 V for the second are used as input signal for simulation. Figures 10 and 11 give the frequency responses of both tested actuators. A simple state-of-the-art eddy current model, consisting of a constant resistor in parallel to the coil inductance, was introduced in the simulation model.

Obviously, the stroke amplitude and phase shift are well represented in the measured frequency range. Test data at higher frequencies show unsteady behaviour due to statistical friction effects, making a comparison of measurement and simulation impossible. Due to differing design of the two testing devices, friction behaviour
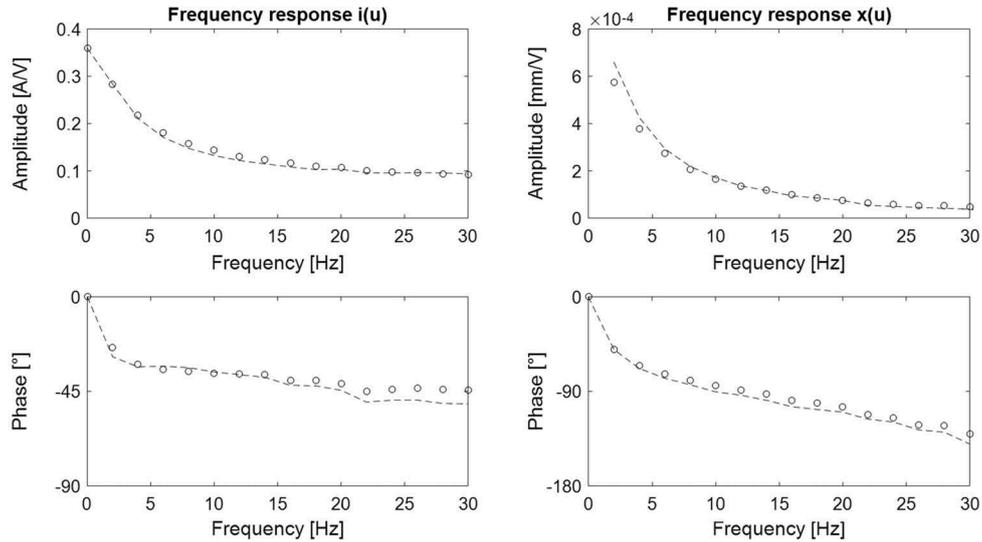
Figure 10. Frequency response of test device 1; points: measurement, lines: simulation.
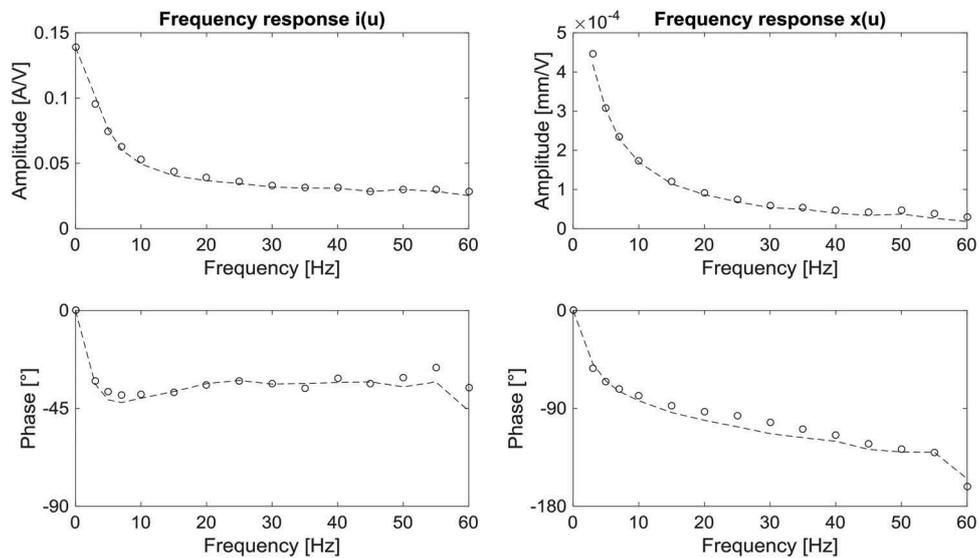

Figure 11. Frequency response of test device 2; points: measurement, lines: simulation.

of device 2 is less pronounced and up to 60 Hz, reproducible measurements are possible. It is obvious that a good accordance between measurement data and simulation exists enabling not only the representation of the measured status quo but furthermore detailed parameter studies due to the physical coupling of all relevant subsystems.

Furthermore, the mathematical model and its realisation in MATLAB Simulink are computationally efficient. Using one core with a clock speed of 2.8 GHz and a fixed step size of $2 \cdot 10^{-5}$ s, the actuator model including its mechanics achieves real-time performance. The included closed algebraic loop resulting from the eddy current model requires almost 50% of the calculation time.

Conclusion and outlook

In the scope of this paper, a novel lumped-parameter model for proportional magnets is derived and validated by means of simulation and measurement results. Starting with the fundamental equations for such actuators, state-of-the-art models are analysed. In contrast to the existing phenomenological models, the introduced approach is physically motivated and thus enables parameter studies respecting the most significant fundamental correlations on parameter change. This is achieved by use of approximating functions for the static force characteristics inherently possessing the required shape. This enables analytical calculation of the fundamental differential equations

for deducing the flux linkage characteristics out of the given force equation. Besides a good accordance between reference data and modelled static characteristics, it was demonstrated that in dynamic applications, a good accordance between measurement data and model is achieved.

Nevertheless, further work has to focus on the friction behaviour in such actuators, as radial forces between armature and iron core strongly influence the actuators' performance. Enhanced with such a friction model, the presented approach enables dither and control optimisation in lumped-parameter simulation with high accuracy and especially highly accurate parameter studies e.g. for tolerance analysis or DoE purposes retaining physical correctness on parameter change.

Nomenclature

A	Cross section	[m^2]
F	Magnetic force	[N]
$f(n, i)$	Switching function	[-]
$g(L_0/\lambda_{max}, i)$	Switching function	[-]
$h(u_L, t)$	Eddy current function	[A]
i	Current	[A]
i_R	Restoring current	[A]
i_d	Dissipating current	[A]
$k(x)$	Polynomial function	[N/A]
$k_{0...m}$	Polynomial coefficients of $k(x)$	[N/(A m^n)]
L_0, L_M, L	Inductance	[H]
N	Number of windings	[-]
n	Scaling factor of $g(n, i)$	[-]
m	Degree of polynomial $k(x)$	[-]
$pi_{n,m}$	Polynomial coefficients	[AWb^{n}m^{-m}]
$pf_{n,m}$	Polynomial coefficients	[NA^{n}m^{-m}]
R_M	Magnetic resistance	[A/Wb]
R	Ohmic resistance	[Ω]
t	Time	[s]
u	Voltage	[V]
u_L	Inductive voltage	[V]
W	Electric energy	[J]
W_{mag}	Stored magnetic energy	[J]
W_{mech}	Mechanical energy	[J]
x	Stroke	[m]
x_0	Reference position	[m]
x_M	Measurement position	[m]
λ	Flux linkage	[Wb]
λ_0	Flux linkage in position x_0	[Wb]
λ_{max}	Flux linkage in saturation	[Wb]
μ_0	Permeability	[H/m]

Disclosure statement

No potential conflict of interest was reported by the author.

Funding

Notes on contributor

Olivier Reinertz was born on 4 October 1984 in Eupen, Belgium. He received his diploma and his doctoral degree in mechanical engineering from RWTH Aachen University, Germany. Currently, he is Scientific Director at the Institute for Fluid Power Drives and Systems (IFAS) of RWTH Aachen University. His research focuses on fluid mechatronic devices and multi-domain simulation of fluid power systems.

References

Backé, W. and Klein, A., 2004. Fluid power actuators. *In*: H. Janocha, eds. *Actuators – basics and applications*. 1st ed. Berlin: Springer, 155–230.

Burget, W. and Weber, J., 2012. *Mobile systems – markets, industrial needs and technological trends. In*: Proceedings of the 8th international conference on fluid power (8tn IFK), Dresden, 2, pp. 23–54.

Chua, L.O. and Stromsmoe, K.A., 1970. Lumped-circuit models for nonlinear inductors exhibiting hysteresis loops. *IEEE transactions on circuit theory*, 17 (4), 564–574. doi:10.1109/TCT.1970.1083192

Cristofori, D. and Vacca, A., 2012. The modeling of electrohydraulic proportional valves. *Journal of dynamic systems, measurement, and control*, 134, 120–125.

Dell'Amico, A. and Krus, P., 2016. Modelling and experimental validation of a nonlinear proportional solenoid pressure control valve. *International journal of fluid power*, 17 (2), 90–101. doi:10.1080/14399776.2016.1141636

Huayong, Y., *et al.* 2009. Electro-hydraulic proportional control of thrust system for shield tunneling machine. *Automation in construction*, 18 (7), 950–956. doi:10.1016/j.autcon.2009.04.005

Kallenbach, E. *et al.*, 2012. *Elektromagnete - grundlagen, berechnung, entwurf und anwendung*. 4th ed. Wiesbaden: Vieweg+Teubner.

Krimpmann, C., *et al.*, 2016. Simulationsgestützte optimierung von gleitzustandsreglern für hydraulische wegeventile (simulation-based optimization of a sliding mode controller for directional valves). *at – automatisierungstechnik*, 64 (6), 443–456. doi:10.1515/auto-2016-0017

Meng, F., *et al.*, 2016. System modeling, coupling analysis, and experimental validation of a proportional pressure valve with pulsewidth modulation control. *IEEE/ASME transactions on mechatronics*, 21 (3), 1742–1753. doi:10.1109/TMECH.2015.2499270

Roters, H.C., 1941. *Electromagnetic devices*. 1st. New York: John Wiley & Sons.

Ruderman, M. and Gadyuchko, A., 2013. *Phenomenological modeling and measurement of proportional solenoid with stroke-dependent magnetic hysteresis characteristic*. Proceedings of the IEEE International Conference on Mechatronics (ICM), Vicenza, pp. 180–185 doi:10.1007/s00508-013-0342-2

Schultz, A. and Tappe, P., 2006. *The method of finite elements in the design process of valve solenoids*. Proceedings of the 5th International Conference on Fluid Power (5th IFK), Aachen, pp. 315–327.

Vaughan, N.D. and Gamble, J.B., 1996. The modeling and simulation of a proportional solenoid valve. *Journal of dynamic systems, measurement, and control*, 118, 120–125.

Zavarehi, M.K. and Lawrence, P.D., 1999. Nonlinear modeling and validation of solenoid-controlled pilot-operated servovalves. *IEEE/ASME transactions on mechatronics*, 4 (3), 324–334. doi:10.1109/3516.789690